Latin American Journal of Aquatic Research, 53(1): 175-185, 2025
DOI: 10.3856/vol53-issue1-fulltext-3210

Short Communication

Oxygen minimum zone variability off Caldera, northern Chile

Nelson Silva[1†], Marcela Cornejo-D'Ottone[1,2] & Claudia Rozas[1]
[1]Escuela de Ciencias del Mar, Pontificia Universidad Católica de Valparaíso, Valparaíso, Chile
[2]Núcleo Milenio para el Estudio de la Desoxigenación del Océano Pacífico Sur Oriental (DEOXS)
Pontificia Universidad Católica de Valparaíso, Valparaíso, Chile
Corresponding author: Marcela Cornejo-D'Ottone (marcela.cornejo@pucv.cl)

ABSTRACT. Several studies show the increase and intensification of oxygen minimum zones (OMZs) in the eastern edge upwelling systems. However, the models differ from *in situ* measurements. Additionally, Eastern Boundary Upwelling Systems (EBUS) are subject to interannual and interdecadal variability due to phenomena such as El Niño-Southern Oscillation (ENSO). In this work, we analyze the transoceanic information of dissolved oxygen, temperature, and salinity from six cruises with stations between the coast and 82°W at 27-28°S between 1967 and 2022. During the whole period, the study area presented Equatorial Subsurface Water (ESSW), which deepened and decreased its presence away from the coast, while its temperature and salinity decreased and the concentration of dissolved oxygen increased. The ESSW hosted an intense OMZ close to the coast with the highest zonal coverage during strong El Niño (2015). However, no statistically significant relationships were observed between the Oceanic Nino Index and OMZ or oxygen variability in the ESSW. Nevertheless, the temporal oxygen variability showed different patterns, with a decrease in the most oceanic zone (west of 79°W), no trend between 78 and 75°W, a decrease from 1967 to 2000 and then an increment, between 74 and 72°W, and no trend at 71°W.

Keywords: oxygen minimum zone; deoxygenation; equatorial subsurface water; eastern south Pacific; ENSO

The subsurface low dissolved oxygen (DO) content (<1 mL L^{-1}) is one of the most notable oceanographic features of the eastern South Pacific. This characteristic, which also occurs in the other Eastern Boundary Upwelling Systems (EBUS), the eastern North Pacific, and the Arabian Sea, is called oxygen minimum zones (OMZ). The EBUS-OMZ results from DO consumption from aerobic organic matter remineralization, sinking from the highly productive surface layer, slow circulation, and long residence time (Czeschel et al. 2011). Due to the chemically reduced conditions of the OMZs, the anaerobic processes using fixed nitrogen and transforming it into gaseous species (i.e. anammox and denitrification) are active, resulting in ~50% of the nitrogen lost in the ocean. The eastern south Pacific (ESP)-OMZ is the most extensive, shallow, and intense (Morales et al. 1999, Ulloa & Pantoja 2009), responding to the high primary production of the surface layer (Daneri et al. 2000), with a longitudinal extension from 0 to 38°S transported by the Peru-Chile undercurrent. Latitudinally, the OMZ off Callao, Peru (12°S) extends from the coast to ~120°W, reaching depths between 50 and 1,100 m, while off Caldera, northern Chile (27°S) to about 90°W, with depths from 50 to 600 m. In its nucleus, centered around 200 m, the DO reaches concentrations lower than 0.01 mL L^{-1} (Wyrtki 1962, Fuenzalida et al. 2009, Revsbech et al. 2009, Silva et al. 2009). Vertically, the Equatorial Subsurface Water (ESSW) is localized below the Subtropical Water (STW) mass in the north, and Subantarctic Water (SAAW) mass in the south and above the Antarctic Intermediate Water (AAIW) mass. ESSW mixes with SAAW and AAIW as it moves south, increasing its DO at concentrations with a no distinguishable OMZ south of 38°S. The seasonal and interannual variability of the current intensity produces water mass fluctuation (Shaffer et al. 1999), resulting in different participation proportions in a particular

Associate Editor: Juan Placencia

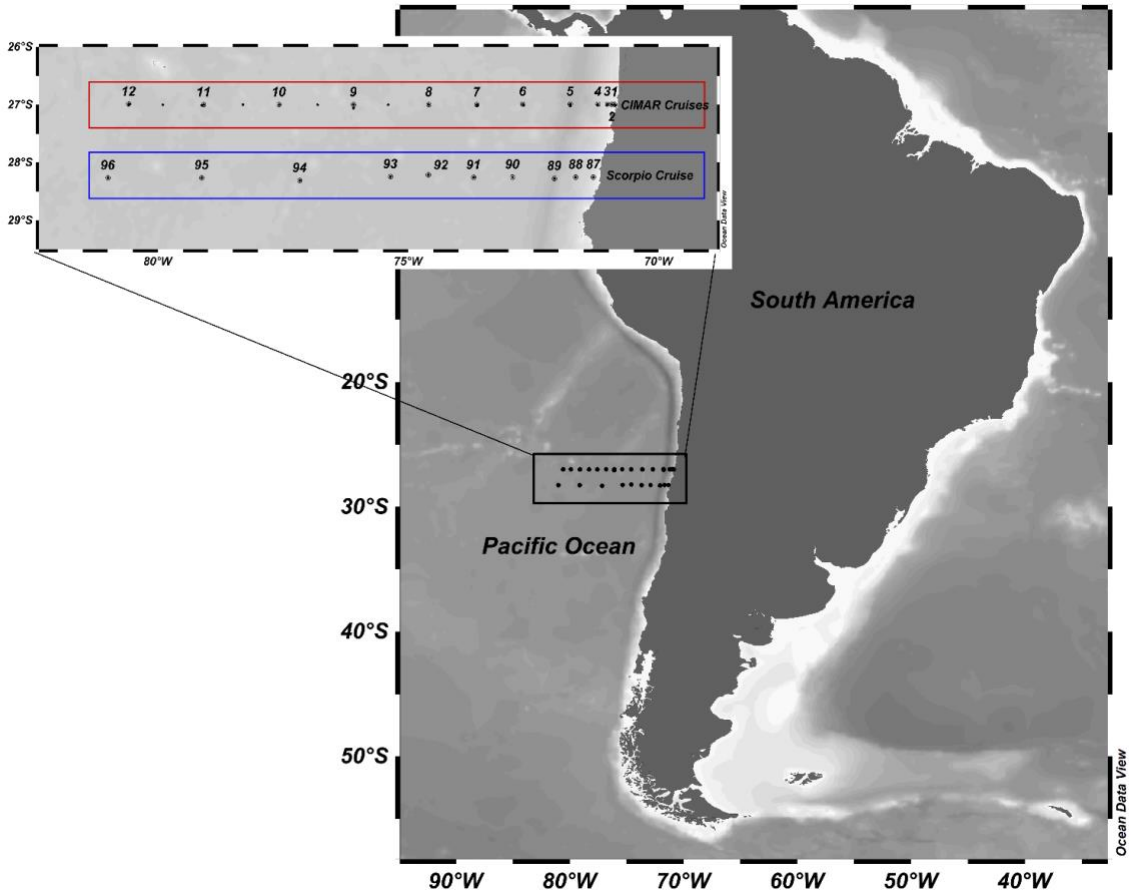

Figure 1. Study region station location during CIMAR cruises 5, 6, 21, 22, and 26 (points in blue square), and Scorpio cruise (points in red square).

place and modifying the DO content of the OMZ (Cornejo et al. 2007). Among these variations, the various stages of the El Niño-Southern Oscillation (ENSO), i.e. El Niño, La Niña, and neutral periods, have generated changes in the volume and DO concentration of the OMZs off the northern coast of Chile and Perú (Morales et al. 1999, Ulloa et al. 2001, Graco et al. 2017). In the last decades, the OMZs have seen experiencing a progressive expansion and decreased DO concentration (Schmidtko et al. 2017, Espinoza-Morriberón et al. 2021), leading to numerous ecological consequences, not only due to the decrease in oxygen and the consequent reduction of habitat for organisms that require oxygen to survive (Limburg et al. 2020) but also due to the effects produced by anaerobic processes in these regions and the decrease in fixed nitrogen, among others (Gruber et al. 2021). However, one of the limitations to understanding the dynamics of the OMZ off the north coast of Chile has been the lack of observations with a sufficient spatio-temporal resolution to evaluate its expansion and seasonal and annual variability.

In the present work, we study the vertical and zonal distribution of the OMZ off Caldera, northern Chile (27-28°S, Fig. 1), and its association with the ESSW. The analysis includes a description of the variation of DO and the development of suboxic zones in the OMZ. The oceanographic research considered two zonal cross-shore transects (at 27 and 28°S) from the coast to 82°W (1,200 km) and from the surface to 1,000 m (Table 1) visited in six cruises. The transects cover the area where the OMZ occurs, and the ESSW has a higher participation percentage (>50%). Further to the west, this body of water is no longer predominant, and the DO is higher than 1 mL L^{-1}. The participation percentage of the water masses was calculated using the mixing triangle method (Silva et al. 2009). Additionally, the coverage (km^2) of the suboxic zone was estimated as a tracer of the OMZ intensity, considering those depths with DO lower than 0.5 mL L^{-1}.

Table 1. Climatic indexes during cruises, temperature, salinity, and oxygen in the Equatorial Subsurface Water (ESSW), zonal extension and coverage area of the oxygen minimum zone (OMZ), and suboxic zone in each cruise. ONI: Oceanic Nino Index, ENSO: El Niño-Southern Oscillation.

Cruise	Scorpio	CIMAR 5	CIMAR 6	CIMAR 21	CIMAR 22	CIMAR 26
Date	May 1967	October 1999	October 2000	October 2015	October 2016	June 2022
ONI (at the date; three months before)	-0.2;-0.5	-1.3;-1.1	-0.6;-0.6	2.4; 1.5	-0.7; -0.3	-0.7;-1.1
ENSO period (at the date; three months before)	Normal	Moderate La Niña	Weak La Niña	Strong El Niño	Weak La Niña	Weak La Niña
ESSW characteristics						
Temperature average ± standard deviation (°C, range)	10.06 ± 1.33 (7.67-12.52)	9.96 ± 1.31 (7.63-12.78)	9.87 ± 1.27 (7.60-12.74)	10.19 ± 1.36 (7.67-13.88)	10.00 ± 1.31 (7.61-12.71)	9.98 ± 1.45 (7.69-12.71)
Salinity average ± standard deviation (range)	34.605 ± 0.117 (34.37-34.81)	34.574 ± 0.088 (34.37-34.75)	34.592 ± 0.077 (34.35-34.74)	34.593 ± 0.100 (34.36-34.83)	34.597 ± 0.088 (34.37-34.80)	34.573 ± 0.107 (34.35-34.85)
Oxygen average ± standard deviation (range)	0.84 ± 0.78 (0.05-2.82)	1.29 ± 0.57 (0.43-3.82)	0.84 ± 0.66 (0.10-4.99)	0.79 ± 0.60 (0.17-3.30)	0.88 ± 0.57 (0.17-3.49)	0.79 ± 1.34 (0.09-3.02)
ESSW area (km^{-2})	236.0	218.2	275.1	277.3	276.6	213.3
Oxygen minimum zone						
Zonal extension	76.5°W 590 km	75°W 400 km	81°W 1000 km	81°W 1000 km	79.3°W 800 km	79.0°W 915 km
Area (km^2)	140.5	48.4	192.0	194.5	123.2	141.2
Oxygen inventory in the OMZ (mmol m^{-2})	500	427	615	666	512	331
Suboxic zone area (km^2)	79.5	10.7	105.7	96.9	29.6	81.6

The cruises considered were: Scorpio (1967), which made a transpacific section along 28°S and CIMAR 5 (1999), 6 (2000), 21 (2015), 22 (2016), and 26 (2022) Oceanic islands along 27°S (from the coast to 82°W). Except for Scorpio, which recorded temperature using inversion thermometers and collected discrete samples with Nansen bottles (Reid 1973), continuous temperature, salinity, and DO measurements were made at each oceanographic station using a CTD-O. In addition, for CIMAR cruises, seawater samples were taken to measure DO at standard depths using a rosette equipped with 24 Niskin bottles. The DO analysis was carried out onboard using the Winkler method modified by Carpenter (1965). The DO data from the CTD-O were contrasted and linearly corrected with the discrete Winkler data from each station. The oceanographic variables were correlated with ENSO, considering the Oceanic Nino Index (ONI) obtained from https://origin.cpc.ncep.noaa.gov/.

The transect shows the presence of the ESSW along the studied period, covering an area (longitude in km × depth) ranging between 213.3 and 277.3 km^2. The highest presence of the ESSW was observed close to the coast, reaching up to 93% of participation. The ESSW decreased westward participation and the zonal and vertical extension (Fig. 3). The maximum area coverage was observed during CIMAR 21 (year 2021), while the minimum was observed during CIMAR 26 (year 2022) (Table 1). The ESSW participation percentage typically decreased offshore, with no decreasing or increasing temporal trend (Table 1). In addition, nuclei with greater participation of ESSW were observed to be separated from the coastal core. These cores have been identified as mesoscale eddies (>50 km in diameter) that transport waters with low oxygen content from the coast, which can last for months, intensifying the reduced conditions of the OMZ differentiated from the surrounding waters (Cornejo et al. 2016, Andrade et al. 2017).

The ESSW transports southward the OMZ, mainly in the coastal region. However, although the OMZ was observed throughout the whole study period inside the ESSW, there was no significant correlation between zonal coverage (Figs. 2-3). The lowest zonal OMZ extension was observed in Scorpio (year 1967; up to 76.5°W and 590 km) and CIMAR 5 (year 1999; up to

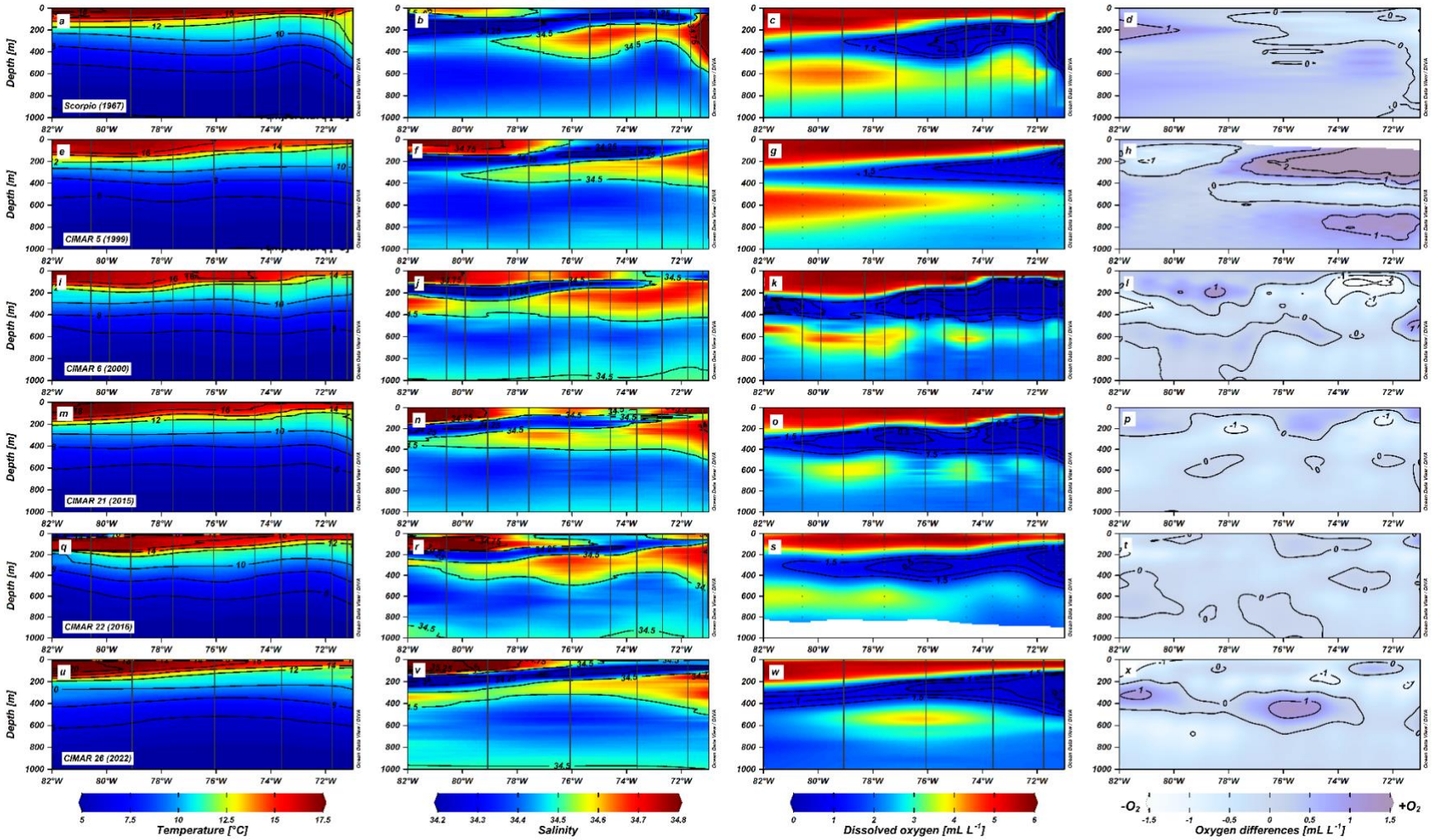

Figure 2. Vertical distribution of temperature (a, e, i, m, q, u), salinity (b, f, j, n, r, v), dissolved oxygen (c, g, k, o, s, w), and oxygen differences (d, h, l, p, t, x) along the cross-shore transect off Caldera (27°S), northern Chile, in six cruises: Scorpio (first file), CIMAR 5 (second file), CIMAR 6 (third file), CIMAR 21 (fourth file), CIMAR 22 (fifth file), and CIMAR 26 (sixth file)

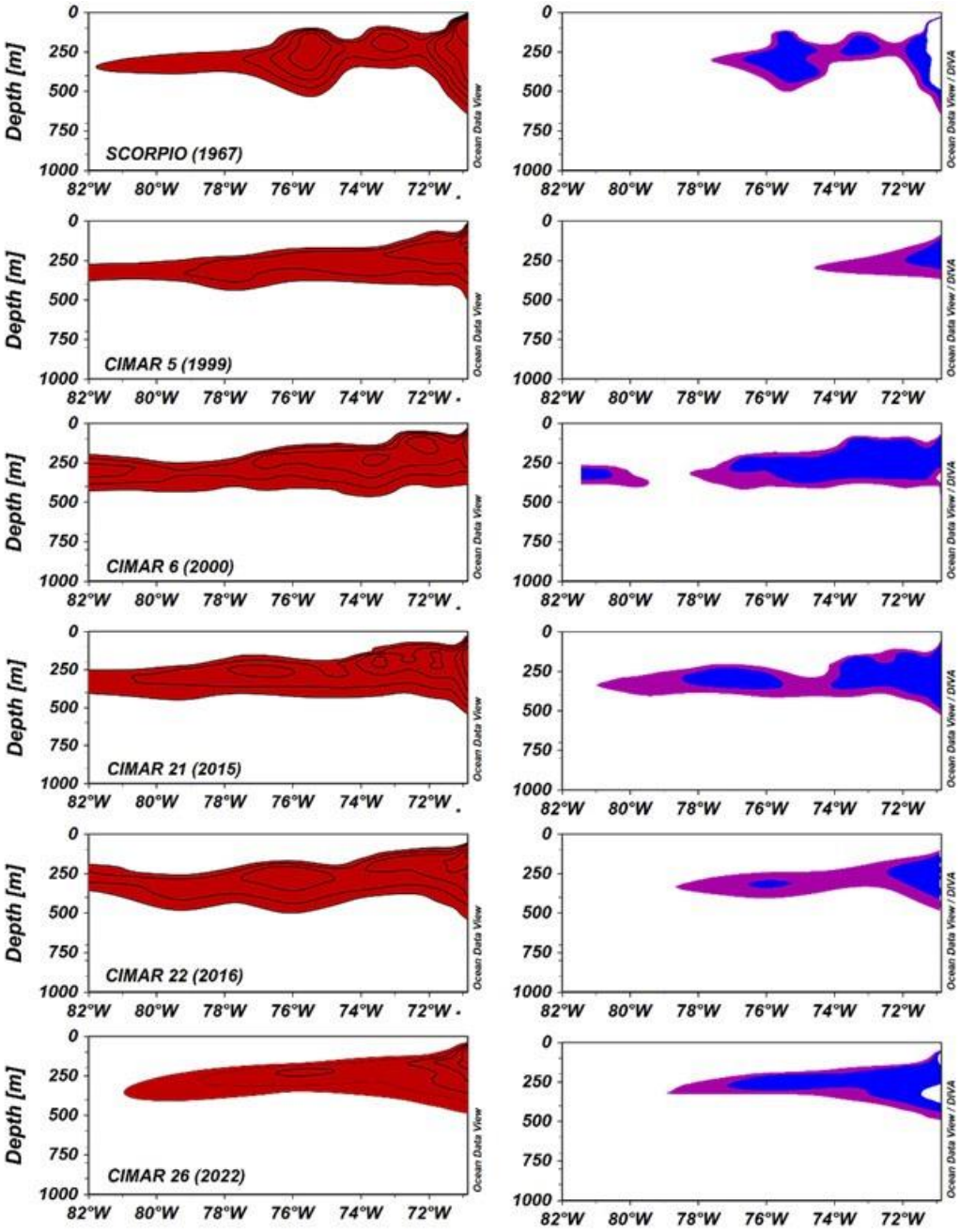

Figure 3. Zonal coverage of the Equatorial Subsurface Water (ESSW) (>50% participation percentage; left column) and presence of oxygen minimum zone (OMZ) (purple region) and suboxic zone (blue region) (right column) in the six cruises along the 27-28°S.

75°W and 400 km), while the largest was in CIMAR 6 and CIMAR 21 (years 2000 and 2015; in both cruises up to 81°W and 1,000 km) (Table 1). Due to the different OMZ vertical thicknesses, its coverage area does not necessarily coincide with the most extended zonal extension. Thus, the lowest coverage was observed on CIMAR 5 (1999), while the highest during CIMAR 21 (2015). The highest OMZ zonal extension and area coverage during CIMAR 21 (up to 81°W with coverage of 194.5 km^2) was developed under one of the strongest El Niño events in recent decades (ONI: 2.4; Fig. 4). During this cruise, the temperature in the ESSW reached up to 13.88°C (average 10.19 ± 1.36°C), the highest values of the whole period. On the contrary, during the weak La Niña (CIMAR 6), the minimum temperature in the ESSW was observed (7.60°C; ave-

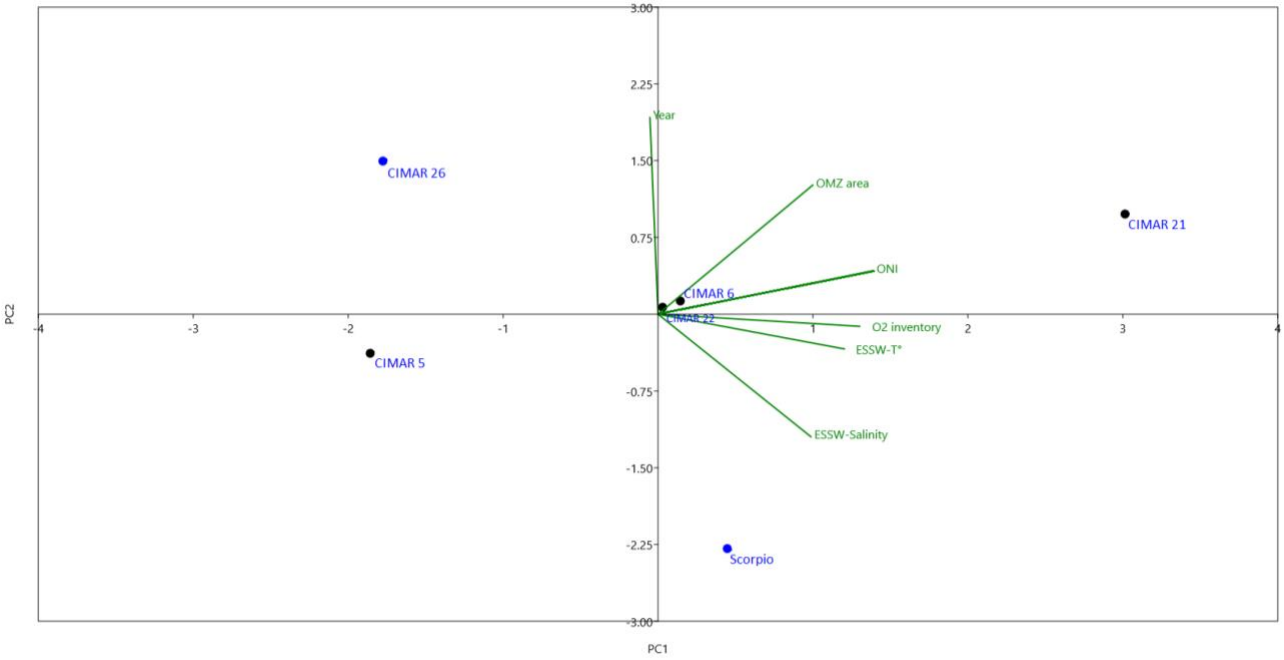

Figure 4. Principal component analysis comparing the physical and chemical properties of the Equatorial Subsurface Water (ESSW) between analyzed cruises.

rage 9.87 ± 1.27°C). The correlation between the ONI and average temperature and maximum temperature shows these patterns (r = 0.84 and 0.90, respectively; $P < 0.05$). This relationship was not observed between the ONI and salinity, neither with OMZ coverage nor the DO average. However, minima and maxima DO values were observed in CIMAR 5 and CIMAR 21 (moderate La Niña and strong El Niño, respectively). Inside the OMZ, a suboxic zone (DO < 0.5 mL L^{-1}) was present during all the cruises, varying its coverage area from 10.7 to 105.7 km^2. This coverage area did not follow the intensity of the ONI (e.g. the lower (higher) coverage was observed during the CIMAR 5 (CIMAR 6) cruise under a moderate (weak) La Niña) (Table 1). A principal component analysis separated the CIMAR 21 characteristics from the rest of the cruises. The first two principal components, PC1 and PC2, explained 84.1% of the total variation in the ESSW and ONI value, and OMZ coverage area accounted for the ESSW variability directly for CIMAR 6, CIMAR 21, and CIMAR 22, while inversely for CIMAR 5. In addition, CIMAR 6 and CIMAR 22 are grouped close to the origin. This correlation reflects different stages for ENSO with CIMAR 6 and CIMAR 22 under weak La Niña, CIMAR 5 under moderate La Niña, and CIMAR 21 under strong El Niño. In contrast, salinity and temperature were significant for the Scorpio cruise and CIMAR 26. Unlike the previous CIMARs cruises conducted in October, Scorpio and CIMAR 6 developed in May and June, respectively, although under two different ENSO stages, normal and weak La Niña, respectively (Fig. 4). Thus, the PCA results suggest that ESSW also experiences seasonal changes and interannual variability, which can modify its physical and oxygen characteristics.

The DO anomalies (delta DO; DO concentration minus average DO concentration considering the six cruises for each depth) (Figs. 2d, h, l, p, t, x) show higher and lower delta DO patterns during the study period. Thus, the delta DO distribution shows higher variability during CIMAR 5 (year 1999) under moderate La Niña along the whole transect, with a DO average concentration ranging from 45 to 75% higher than the rest of the studied period, while the higher negative delta DO was observed during CIMAR 6 (year 2000) although the average DO in the ESSW was not, the lower of the six cruises. According to these results and to define the trend of DO along the 27°S transect, its variability at 26.5 kg m^{-3} (the core of the ESSW) was analyzed spatially, every 1° of longitude from the coast to 82°W (Figs. 5a-c), and temporarily, through the cruises (Figs. 5d-f). While the temperature and salinity decreased offshore (Figs. 5a-b), the average DO concentrations increased (Fig. 5c) due to the lower ESSW participation. The zonal DO distribution shows higher concentrations during Scorpio (1967) at 82°W,

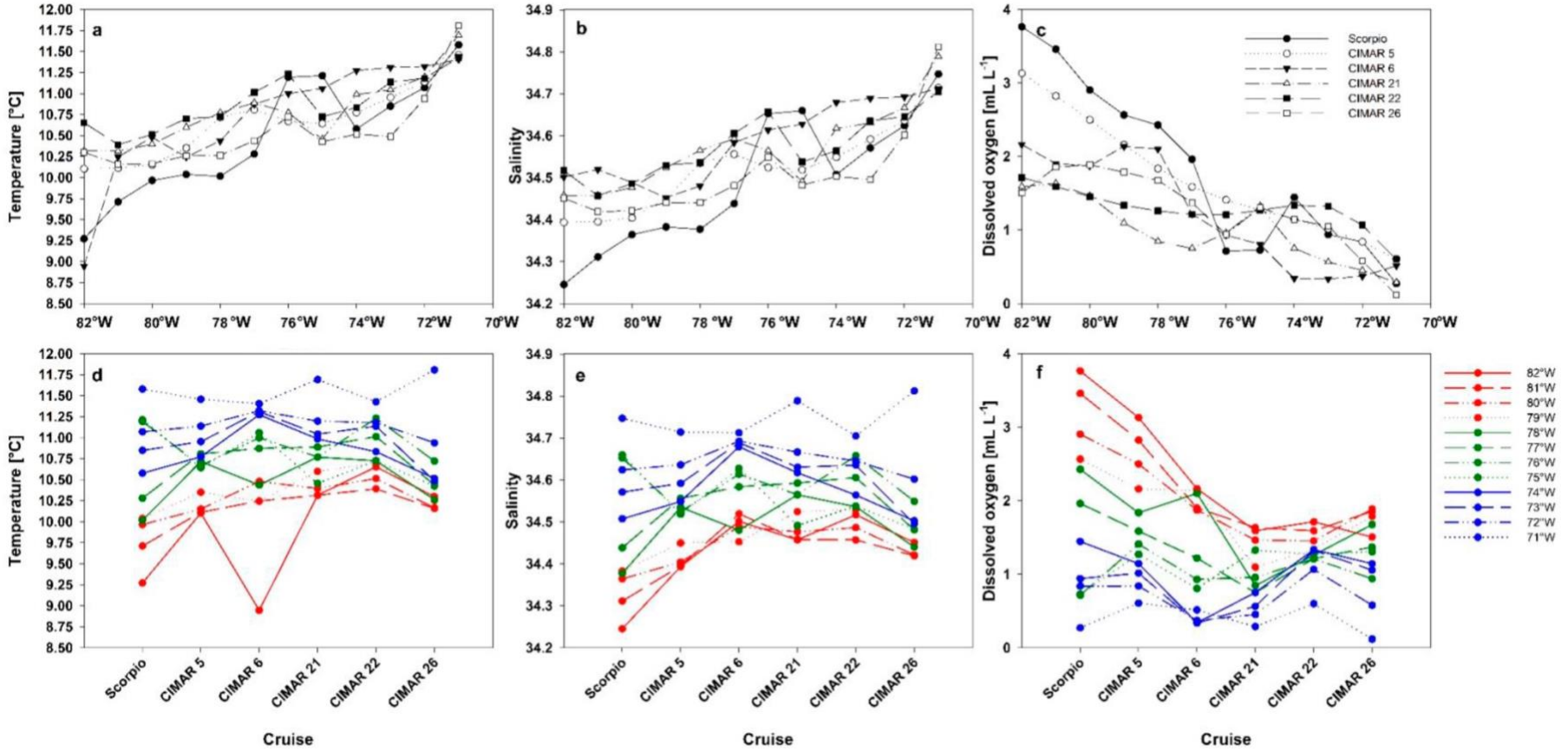

Figure 5. Zonal and average value at 26.5 kg m^{-3} of temperature (a, d), salinity (b, e), and dissolved oxygen concentration (c, f) every 1° of longitude between 82 and 71°W during the six cruises (Scorpio, CIMAR 5, CIMAR 6, CIMAR 21, CIMAR 22, and CIMAR 26).

almost 2 mL L^{-1} higher than in CIMAR 26 (2022); this DO trend and difference among cruises decreased towards the coast (Fig. 5c). However, the 1° longitude distribution shows a different trend among cruises for each variable. Thus, four types of DO distributions could be distinguished along the transect at different oceanographic regions along the whole studied period (Fig. 5f): i) a significant temporal decreasing DO concentration westward of 79°S (from 0.016 to 0.044 mL L^{-1} yr^{-1}) although with a lower decrease the last 10 years; ii) no trend between 78°S and 75°W, iii) a decreasing DO from Scorpio to CIMAR 6, after which the DO concentration increased over time between 74 and 72°W, both trends with little data to be statistically significant; and iv) no trend at 71°W. The DO decreasing trend was not accompanied by any trend for temperature and salinity, such as observed in the global ocean (Ito et al. 2022), suggesting that no physical property changes modifying the solubility at the water mass formation are responsible for the lower oxygen concentrations. In addition, the DO decline observed in the oceanic region agrees with the decline trend reported at 150 m depth in the coastal upwelling region off Perú (10 µmol kg^{-1} $decade^{-1}$ or ~0.023 mL L^{-1} yr^{-1}; Espinoza-Morriberón et al. 2021). Thus, although no OMZ expansion was observed during the period, and DO is still high in the oceanic region, its decrease in DO can stimulate N_2O production by nitrification and reactive nitrogen loss (Oschlies et al. 2018). In addition, the rate of oxygen decline in the oceanic zone is considerably higher than the 2% decline previously reported (Schmidtko et al. 2017). This decrease is between 30 and 60% considering the decrease between the CIMAR 26 (2022) and Scorpio (1967) cruises, while between 9 and 52% considering the difference between CIMAR 26 (CIMAR 22) and CIMAR 5 (1999), being one-fold higher than the modeled for 300 m (Oschlies et al. 2017).

Finally, the coastal and oceanic OMZ temporal variability, surface characteristics, and DO-associated characteristics were compared (i.e. mixed layer, sea surface temperature (SST), and salinity, oxygen gradient in oxycline, the upper limit of the OMZ, vertical extension of the OMZ, and DO budget in the

Table 2. Physics and oxygen characteristics of the water column of two stations, coastal and oceanic, during the cruises. OMZ: oxygen minimum zone, MLD: mixed layer depth, DO: dissolved oxygen. nd: not determined. *First measurement at 10 m.

Cruise	Scorpio	CIMAR 5	CIMAR 6	CIMAR 21	CIMAR 22	CIMAR 26
Coastal station (71°48'W)						
Station	88	5	74	5	5	5
MLD (m)	41	34	44	28	5	55
Surface temperature (°C)	16.8	14.4	14.2	16	16.3	15
Surface salinity average	34.53	34.47	34.44	34.74	34.64	34.46
Surface oxygen mean (mL L^{-1})	5.6	6.2	6	5.7	5.7*	5.6
DO gradient at the oxycline (mL L^{-1} m^{-1})	-0.096	-0.093	-0.179	-0.065	-0.053	-0.057
OMZ upper boundary (m)	136	140	94	119	125	137
OMZ thick (m)	260	195	303	308	305	294
Oxygen inventory at the OMZ (mmol m^2)	120	135	109	119	160	106
Oceanic station (80°34'W)						
Station	96	12	63	12	12	11b (79°6'W)
MLD (m)	41	54	83	9	45	105
Surface temperature (°C)	17.9	17.1	17	18.1	17.6	17.32
Surface salinity average	34.57	34.79	34.83	34.88	34.84	34.89
Surface oxygen mean (mL L^{-1})	5.5	5.6	5.7	5.5	5.6	5.43
DO gradient at the oxycline (mL L^{-1} m^{-1})	nd	-0.018	-0.034	-0.021	-0.032	-0.029
OMZ upper boundary (m)	No OMZ	No OMZ	275	327	No OMZ	318
OMZ thick (m)	0	0	115	23	0	4
Oxygen inventory at the OMZ (mmol m^2)	No OMZ	No OMZ	78.8	21.6	No OMZ	3.9

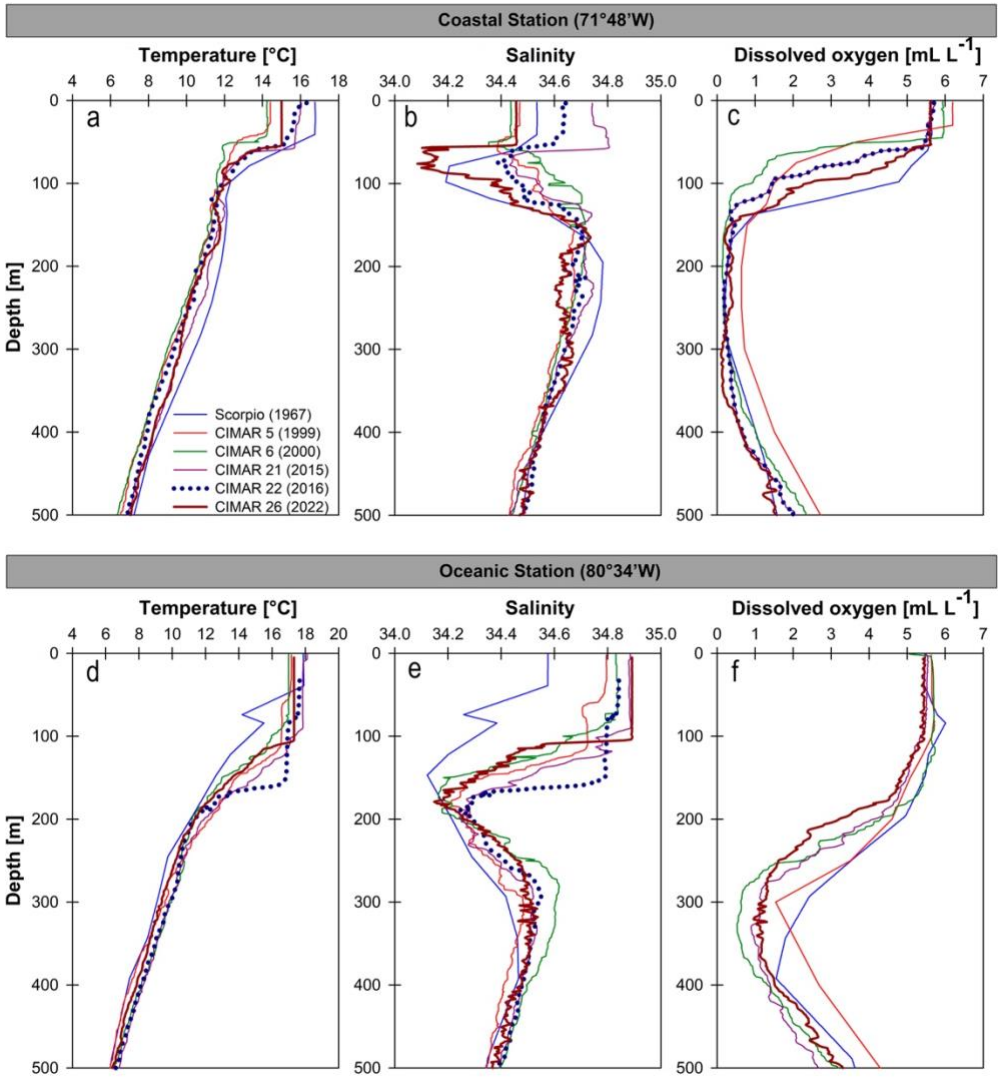

Figure 6. Vertical distribution of temperature (a, d), salinity (b, e), and dissolved oxygen (c, f) at a coastal (71°48'W) and an oceanic (80°34'W) off Caldera (27°S), northern Chile, during: Scorpio (blue line), CIMAR 5 (red line), CIMAR 6 (green line), CIMAR 21 (purple line), CIMAR 22 (black dotted line), and CIMAR 26 (brown line).

OMZ) in two stations, at 71.8 and 80.6°W, sampled repeatedly in every cruise (Table 2, Fig. 6). The mixed layer depth (MLD), the (SST), and sea surface salinity (SSS) presented higher values in the oceanic station than in the coastal station. Espinoza-Morriberón et al. (2021) tend to shallow the oxycline on Peru's coasts, coinciding with the deoxygenation observed in that upwelling system. However, no decreasing or increasing trends were observed throughout the studied period for oxycline, OMZ upper boundary, DO gradient at the oxycline, MLD, SST, and SSS, or between them and the ONI. Regarding the OMZ, the coastal station presented the thickest OMZ (308 m) of the entire period. Nevertheless, the upper boundary and oxygen inventory of the OMZ were not characteristic of the other cruises. However, only three cruises presented OMZ at the oceanic station, of which the deepest occurred during El Niño (327 m). However, its thickness was considerably lower than that observed in CIMAR 6, where OMZ thickness was 115 m (Table 2).

These results confirm a DO decline in the oceanic region of the eastern South Pacific Ocean off Caldera (27°S) in the core of the ESSW in the last decades, with increasing rates offshore. These rates are higher than the previously reported. However, the rates and trends change when considering shallower and deeper depths and toward the coast. More monitoring is required to determine, explain, and understand the DO rates.

Credit author contribution

N. Silva: funding acquisition, project administration, conceptualization, methodology, writing-original draft; M. Cornejo-D'Ottone: funding acquisition, project administration, conceptualization, methodology, analysis, writing-original draft, review, editing; C. Rozas: methodology, review, editing. All authors have read and accepted the published version of the manuscript.

Conflict of interest

The authors declare no potential conflict of interest in this manuscript.

ACKNOWLEDGMENTS

The authors thank the crew of AGOR-60 Vidal Gormaz and AGS 61 Cabo de Hornos, where CIMAR cruises were conducted. This work is a contribution of the CIMAR 21 (CONA C21IO 15-03 and C21IO 15-09), CIMAR 22 (C22IO 16-03 and C22IO 16-10), and CIMAR 26 (CONA C26IO22-01) projects and Núcleo Milenio para el estudio de la Desoxigenación en el Océano Pacífico Sur Oriental (DEOXS; NCN 2024_113). To Constanza Hernández, Paola Reinoso and Francisco Gallardo for their sampling and nutrient analysis work.

REFERENCES

Andrade, I., Hormazábal, S. & Combes, V. 2017. Intrathermocline eddies at the Juan Fernández Archipelago, southeastern Pacific Ocean. Latin American Journal of Aquatic Research, 42: 888-906. doi: 10.3856/vol42-issue4-fulltext-14

Carpenter, J.H. 1965. The Chesapeake Bay Institute technique for the Winkler dissolved oxygen method. Limnology and Oceanography, 10: 141-143. doi: 10.4319/lo.1965.10.1.0141

Cornejo, M., Farías, L. & Gallegos, M. 2007. Seasonal cycle of N_2O vertical distribution and air-sea fluxes over the continental shelf waters off central Chile (36°S). Progress in Oceanography, 75: 383-395. doi: 10.1016/j.pocean.2007.08.018

Cornejo-D'Ottone, M., Bravo, L., Ramos, M., Pizarro, O., et al. 2016. Biogeochemical characteristics of a long-lived anticyclonic eddy in the eastern South Pacific Ocean. Biogeo-sciences, 13: 2971-2979. doi: 10.5194/bg-13-2971-2016

Czeschel, R., Stramma, L., Schwarzkopf, F.U., Giese, B.S., et al. 2011. Middepth circulation of the eastern tropical South Pacific and its link to the oxygen minimum zone. Journal of Geophysical Research: Oceans, 116: C01015. doi: 10.1029/2010JC006565

Daneri, G., Dellarossa, V., Quiñones, R., Jacob, B., et al. 2000. Primary production and community respiration in the Humboldt Current System off Chile and associated oceanic areas. Marine Ecology Progress Series, 197: 41-49. doi: 10.3354/meps197041

Espinoza-Morriberón, D., Echevin, V., Gutiérrez, D., Tam, J., et al. 2021. Evidence and drivers of ocean deoxygenation off Peru over recent past decades. Scientific Reports, 11: 20292. doi: 10.1038/s41598-021-99876-8

Fuenzalida, R., Schneider, W., Garcés-Vargas, J., Bravo, L., et al. 2009. Vertical and horizontal extension of the oxygen minimum zone in the eastern South Pacific Ocean. Deep Sea Research - Part II: Topical Studies in Oceanography, 56: 992-1003. doi: 10.1016/j.dsr2.2008.11.001

Graco, M.I., Purca, S., Dewitte, B., Castro, C.G., et al. 2017. The OMZ and nutrient features as a signature of interannual and low-frequency variability in the Peruvian upwelling system. Biogeosciences, 14: 4601-4617. doi: 10.5194/bg-14-4601-2017

Gruber, N., Boyd, P.W., Frölicher, T.L. & Vogt, M. 2021. Biogeochemical extremes and compound events in the ocean. Nature, 600: 395-407. doi: 10.1038/s 41586-021-03981-7

Ito, T., Takano, Y., Deutsch, C. & Long, M.C. 2022. Sensitivity of global ocean deoxygenation to vertical and isopycnal mixing in an ocean biogeochemistry model. Global Biogeochemical Cycles, 36: e2021 GB007151. doi: 10.1029/2021GB007151

Limburg, K.E., Breitburg, D., Swaney, D.P. & Jacinto, G. 2020. Ocean deoxygenation: A primer. One Earth, 2: 24-29. doi: 10.1016/j.oneear.2020.01.001

Morales, C.E., Hormazábal, S.E. & Blanco, J. 1999. Interannual variability in the mesoscale distribution of the depth of the upper boundary of the oxygen minimum layer off northern Chile (18-24°S): Implications for the pelagic system and biogeochemical cycling. Journal of Marine Research, 57: 909-932. doi: 10.1357/002224099321514097

Oschlies, A., Brandt, P., Stramma, L. & Schmidtko, S. 2018. Drivers and mechanisms of ocean deoxy-genation. Nature Geoscience, 11: 467-473. doi: 10.1038/s41561-018-0152-2

Oschlies, A., Duteil, O., Getzlaff, J., Koeve, W., et al. 2017. Patterns of deoxygenation: sensitivity to natural and anthropogenic drivers. Philosophical Transactions of the Royal Society A, 375: 20160325. doi: 10.1098/rsta.2016.0325

Reid, J.L. 1973. Transpacific hydrographic sections at lats. 43ºS and 28ºS: the Scorpio Expedition-III. Upper water and a note on southward flow at mid-depth. Deep-Sea Research, 20: 39-49. doi: 10.1016/0011-7471(73)90041-7

Revsbech, N.P., Larsen, L.H., Gundersen, J., Dalsgaard, T., et al. 2009. Determination of ultra-low oxygen concentrations in oxygen minimum zones by the STOX sensor. Limnology and Ocea-nography: Methods, 7: 371-381.

Schmidtko, S., Stramma, L. & Visbeck, M. 2017. Decline in global oceanic oxygen content during the past five decades. Nature, 542: 335-339. doi: 10.1038/nature 21399

Shaffer, G.S., Hormazábal, S., Pizarro, O. & Salinas, S. 1999. Seasonal and interannual variability of currents and temperature off central Chile. Journal of Geophysical Research, 104: 29951-29961. doi: 10.1029/1999JC900253

Silva, N., Rojas, N. & Fedele, A. 2009. Water masses in the Humboldt Current System: Properties, distribution, and the nitrate deficit as a chemical water mass tracer for Equatorial Subsurface Water off Chile. Deep Sea Research - Part II: Topical Studies in Oceanography, 56: 1004-1020. doi: 10.1016/j.dsr2. 2008.12.013

Ulloa, O. & Pantoja, S. 2009. The oxygen minimum zone of the Eastern South Pacific. Deep Sea Research- Part II, 56: 987-991. doi: 10.1016/j.dsr2.2008.12.004

Ulloa, O., Escribano, R., Hormazabal, S., Quinones, R.A., et al. 2001. Evolution and biological effects of the 1997-98 El Niño in the upwelling ecosystem off northern Chile. Geophysical Research Letters, 28: 1591-1594.

Wyrtki, K. 1962. The subsurface water masses in the western South Pacific Ocean. Australian Journal of Marine and Freshwater Research, 13: 18-47. doi: 10.1071/MF9620018

Received: January 23, 2024; Accepted: September 24, 2024